

Absolute cross sections for dissociative electron attachment to condensed CH₃Cl and CH₃Br: Effects of potential energy curve crossing and capture probability

P. Ayotte, J. Gamache, A. D. Bass, I. I. Fabrikant, and L. Sanche

Citation: *The Journal of Chemical Physics* **106**, 749 (1997); doi: 10.1063/1.473163

View online: <http://dx.doi.org/10.1063/1.473163>

View Table of Contents: <http://scitation.aip.org/content/aip/journal/jcp/106/2?ver=pdfcov>

Published by the [AIP Publishing](#)

Articles you may be interested in

Electron induced dissociation of trimethyl (methylcyclopentadienyl) platinum (IV): Total cross section as a function of incident electron energy

J. Appl. Phys. **106**, 074903 (2009); 10.1063/1.3225091

Condensed-phase effects on absolute cross sections for dissociative electron attachment to CFCs and HCFCs adsorbed on Kr

J. Chem. Phys. **119**, 2658 (2003); 10.1063/1.1587688

Dissociative chemisorption of CH₄ on a cesiated Pt(111) surface studied by supersonic molecular beam scattering techniques

J. Chem. Phys. **116**, 7673 (2002); 10.1063/1.1467051

Giant enhancement of electron-induced dissociation of chlorofluorocarbons coadsorbed with water or ammonia ices: Implications for atmospheric ozone depletion

J. Chem. Phys. **111**, 2861 (1999); 10.1063/1.479613

Low-energy dissociative electron attachment to CFCI₃, CF₂Br₂, and 1,1,1- and 1,1,2-C₂Cl₃F₃: Intermediate lifetimes and decay energetics

J. Chem. Phys. **106**, 9594 (1997); 10.1063/1.473858



Absolute cross sections for dissociative electron attachment to condensed CH₃Cl and CH₃Br: Effects of potential energy curve crossing and capture probability

P. Ayotte,^{a)} J. Gamache, A. D. Bass, I. I. Fabrikant,^{b)} and L. Sanche

Groupe du CRM en Sciences des Radiations, Faculté de médecine, Université de Sherbrooke, Sherbrooke, Québec, Canada J1H 5N4

(Received 20 May 1996; accepted 4 October 1996)

We report cross sections for the trapping of 0–10 eV electrons by CH₃Cl and CH₃Br physisorbed onto a Kr covered Pt substrate, measured as a function of Kr film thickness and methyl halide concentration. The molecules stabilize electrons incident at the surface by the dissociation of transient CH₃Cl[−] and CH₃Br[−] ions into an atomic anion and a neutral fragment [dissociative electron attachment DEA]. For CH₃Cl, the condensed phase absolute DEA cross section at ≈0.5 eV, reaches $13 \times 10^{-18} \text{ cm}^2 \pm 50\%$, which is 10^4 – 10^6 times larger than the gas phase cross section. At higher energies (5–10 eV) for CH₃Cl, our measurements provide a lower limit for the DEA cross section. For CH₃Br, the maximum DEA cross section occurs below the vacuum level; we measure an absolute magnitude of $3.0 \times 10^{-16} \text{ cm}^2 \pm 50\%$ near 0 eV, which is 100 times larger than the corresponding gas phase value. These enhancements in cross section arise from the lowering of the potential energy surfaces of intermediate anions due to polarization induced in the Kr layer and metal substrate. An increase in DEA cross section with a reduction in the distance of transient anions from the metal surface, is explained by the effect of image charges on the energy at which anion and neutral ground state potential energy curves cross. Below thicknesses of 5 ML of Kr, a decrease in DEA cross section is observed and attributed to a reduction in the electron capture probability of the halide due to competition with transfer to the metal substrate. © 1997 American Institute of Physics. [S0021-9606(97)02302-7]

I. INTRODUCTION

It is well established that a transient negative ion formed by the attachment of a low-energy electron to a molecule, can decay either by releasing the captured electron or by forming a stable anion.¹ The latter may result from the dissociation of the transient anion into a neutral radical and stable anion (i.e., dissociative electron attachment) or its stabilization via energy transfer to surrounding media. In this article, we present results on dissociative electron attachment (DEA) to CH₃Cl and CH₃Br condensed onto multilayer Kr films supported by a Pt surface. The distance between the intermediate ions CH₃Cl[−] and CH₃Br[−] and the Pt surface is varied by changing the thickness of the Kr spacer layer which, in turn modifies the influence of the image charge induced in the metal substrate. The formation of stable anions by the impact of 0–10 eV electrons is measured by monitoring the number of anions that remain on the surface using a modified version of the charge trapping (CT) method developed by Marsolais *et al.*² Since the dissociation of a transient anion produces a “resonance” structure in the surface³ and vacuum anion yields,^{4,5} both CT and the electron stimulated desorption (ESD) techniques can provide direct evidence for the occurrence of DEA reactions. In addition, CT provides absolute measurements and so allows

quantitative comparisons between gas and condensed phase results. DEA to CH₃Cl and CH₃Br has been intensively studied in the gas phase and is believed to be responsible for products photogenerated from these molecules absorbed on various surfaces. We therefore first present an overview of existing information in Sec. II. In Sec. III, we explain the CT measurement technique and other experimental details. Our results are presented in Sec. IV. These were recorded at different spacer layer thickness and methyl halide surface concentrations and shows that for both molecules, DEA occurs. In Sec. V, we discuss the present results in terms of mechanisms that can enhance the magnitude of condensed phase DEA relative to the gas phase and explain the behavior of the DEA cross section as a function of the distance between the transient anion and the metal surface. The main results and conclusions are summarized in Sec. VI.

II. REVIEW OF PREVIOUS STUDIES

A. DEA to gaseous CH₃Cl and CH₃Br

DEA to gaseous CH₃Cl and CH₃Br has been investigated with both electron beam and electron swarm techniques. Measurements of the formation of Cl[−] from CH₃Cl^{6–13} have given conflicting results. In fact, the behavior and magnitudes of DEA cross sections measured by electron beam methods,^{9,12} are in substantial disagreement with those derived from swarm data,^{6,8} giving dispersed values of the absolute cross sections which differ by several orders of magnitude. Furthermore, calculations using resonant

^{a)}Present address: Sterling Chemistry Laboratory, Department of Chemistry, Yale University, New Haven, CT 06511.

^{b)}Permanent address: Department of Physics and Astronomy, University of Nebraska, Lincoln, Nebraska 68588-0111.

R-matrix theory¹⁴ give values which are orders of magnitude smaller than the lowest experimental values found at room temperature. Burrow and co-workers^{9,12} have presented evidence on the effects of impurities which lead to an overestimate of the DEA experimental cross sections. There are reports of a narrow peak near 0 eV in the Cl[−] yield function, which, according to Chu and Burrow,⁹ derives from trace impurities of CCl₄ in the sample gas; the extremely large DEA cross section for Cl[−] production from CCl₄ makes measurements near 0 eV, particularly difficult. Subsequently, Pearl and Burrow¹² investigated the temperature dependence of the DEA cross section within the 0–3 eV range. They found that a peak at 0.8 eV, is probably due to HCl impurities produced by reactions on the electron source (i.e., a hot filament). However, at higher temperatures, the Cl[−] signal becomes stronger and at energies lower than 0.8 eV (the DEA threshold for HCl) is believed to correspond to Cl[−] production from CH₃Cl. Calculated cross sections¹⁴ agree reasonably well with the swarm analysis of Datskos and co-workers⁸ for temperatures within the range 700–800 K. Recently closing the debate, Pearl and co-workers found a good agreement between the experimental and theoretical DEA cross sections at 600 K.¹⁵ A further contribution to the yield of Cl[−] and CH₂Cl[−] from CH₃Cl under electron impact^{10–12} is found at about 7.4 eV and has been ascribed to DEA to a higher-lying CH₃Cl[−] state.

There also has been disagreement in the literature^{16–26} regarding the magnitude and energy dependence of electron attachment cross sections in gaseous CH₃Br. Values for the electron attachment rate constants measured within the 0–1 eV range are found to vary by more than three orders of magnitude. These disagreements have been resolved by the work of Datskos, Christophorou, and Carter,²⁶ who performed an electron swarm study on the effect of temperature on DEA to CH₃Br diluted in a buffer of N₂. At room temperature, CH₃Br attaches slow electrons weakly but as the temperature is raised from 300 to 700 K the electron attachment cross section between 0 and 0.9 eV, increases by more than two orders of magnitude. At 300 K, the cross section exhibits a peak at 0.38 eV that shifts to lower energy with increasing temperature.

B. DEA to condensed CH₃Cl and CH₃Br

DEA to condensed CH₃Cl and CH₃Br has recently been investigated by Rowntree *et al.*²⁷ who measured the anion yields desorbed from multilayer films by the impact of 0–12 eV electrons. They measured Cl[−] and H[−] yields for 0.3 monolayers (ML) of CH₃Cl deposited on a Kr substrate and from 3 ML CH₃Cl deposited on Pt. In the latter experiment, their Cl[−] yields exhibit two peaks at about 7 and 9 eV; two peaks are also found in the H[−] yield function around 8 and 10 eV. For submonolayer CH₃Cl on Kr, there are two structures in the Cl[−] yields which correspond to those measured in the pure CH₃Cl film. Electron stimulated desorption of anions from multilayers of CH₃Br deposited on Pt yielded an extremely weak Br[−] signal. The Br[−] yield function has maxima at ~5 and ~8.5 eV whereas that for H[−] desorption

exhibits a maxima at 7 and 9 eV. In both CH₃Cl and CH₃Br, the maxima in the H[−] and Cl[−] yields were ascribed to different transient anion states. Several of these structures were found to have no counterpart in the gas-phase data. The onsets of the Cl[−] ESD yields were also significantly shifted to lower energies relative to gas phase DEA. No signal was observed below 5 and 3 eV from condensed CH₃Cl and CH₃Br, respectively. This indicated either that the DEA cross section is very small or that the dissociation of CH₃Cl[−] or CH₃Br[−] along the CH₃-halogen-anion coordinate does not lead to Cl[−] or Br[−] desorption at these energies. This would occur if insufficient kinetic energy was transferred to the anion to overcome the *surface polarization potential* (i.e., the attraction of anion to the image charge it creates in the Kr film and supporting metal substrate).

Very recently²⁸ we presented a theoretical analysis of DEA to condensed CH₃Cl accompanied by preliminary results on DEA to CH₃Cl condensed on multilayer Kr. The latter were obtained by measuring the CT cross section as a function of electron energy within the range 0–2.5 eV and Kr film thickness. These results, which are reproduced here in more detail, show a very large enhancement in DEA (between 4 and 6 orders of magnitude) due to the change of phase. Prior to this latter work,²⁸ there existed ample indirect evidence from the photochemistry of CH₃Cl and CH₃Br adsorbed on metal and semiconductor surfaces to indicate the presence of DEA reactions in the condensed state near 0 eV. Several authors^{29–39} have proposed that the photostimulated desorption of neutral radicals from condensed CH₃Cl and CH₃Br can be understood in terms of a DEA mechanism. In this case, photoelectrons or subvacuum ‘‘hot’’ electrons attach to the methyl halide and form a transient anion state that dissociates into CH₃ and Cl[−] (or Br[−]). Such a mechanism was first presented by Marsh *et al.*²⁹ to explain the desorbed yield of CH₃ from CH₃Cl condensed onto a metal substrate and exposed to UV radiation. In retrospect, it is interesting that this interpretation was based partially on gas phase data that showed a maximum in the attachment cross section near 0 eV and which are now believed to be incorrect.⁹ Initial studies were followed by those of Jo and White³⁰ who correlated the photoelectron yields dissociation rates for optically transparent CH₃Cl on Pt(111). These measurements confirmed that photoelectrons play a dominant role in the dissociation process. A similar conclusion was reached by Solymosi *et al.*³¹ in their studies of CH₃Cl photochemistry on clean and *K*-promoted Pd(100) surfaces. Later Dixon–Warren, Jensen, and Polanyi³⁹ attempted to provide direct evidence for DEA by measuring Cl[−] emission from CH₃Cl condensed on Ag(111). However, due to an extremely low desorption yield, it was not possible to conclude if this signal arose from a transient methyl chloride anion.

Studies of substrate-electron-mediated photoreactions have been even more numerous in condensed CH₃Br.^{32–38,40} The results obtained with CH₃Br on a brominated Ni(111),³² a Pt(111),^{36–38} an Ag(111),³³ and a GaAs(110)⁴⁰ surface and on Xe spacer layers^{36–38} all indicate that a CH₃Br[−] state is formed at the surface and dissociates into Br[−] and CH₃, with the latter moiety being expelled in vacuum. On GaAs(110),

photofragmentation of the first monolayer of CH₃Br is induced by the tunneling of electrons thermalized at the conduction band minimum, whereas on Pt(111), and Xe-covered Pt(111), photodissociation is believed to arise from DEA of subvacuum photoexcited electrons. Both of these studies therefore imply that the intermediate anion state extends to energies below the vacuum level. On the other hand, the photoreaction dynamics of multilayer CH₃Br³² and CH₃Br supported on spacer layers³³ indicate that the CH₃Br[−] state leading to CH₃ production is also accessible above the vacuum level.

C. State assignment and interpretation of DEA data

The energy, lifetime, and symmetry assignments of the lowest anion state of isolated CH₃Cl have been deduced from electron transmission^{41,42} and electron-energy-loss⁴³ spectroscopy data combined with $X\alpha$ ^{41,42} and *ab initio* stabilization⁴⁴ calculations. The lowest energy state of CH₃Cl[−] has the symmetry ²A₁ and corresponds to electron capture into the lowest unoccupied C–Cl σ^* orbital of the *a*₁ symmetry (⁸a₁). This orbital is strongly antibonding between the carbon and chlorine atoms. The state lies at 3.45 eV above the vacuum level and according to systematic electron transmission and DEA studies of the gas phase monochloroalkanes,⁴¹ possesses too short a lifetime for measurable C–Cl[−] bond dissociation to occur. It is therefore not surprising to find that, within the 0–4 eV range, at room temperature, the Cl[−] signal lies below the limit of detectability in gas-phase experiments and that calculations give extremely small values (10^{−23}–10^{−25} cm²)^{12–15} for the DEA process. The presence of a detectable signal at higher temperatures can be explained by the increase in the population of higher vibrational levels of ground state CH₃Cl that broaden the Franck–Condon (F–C) region.^{8,14,15} Such a mechanism is completely absent at the cryogenic temperatures necessary to perform the condensed phase experiments. Therefore, another mechanism must be invoked to explain the measurable DEA cross section responsible for surface charging by 0–2 eV electrons²⁸ and for the intense methyl production in the condensed phase photoelectron experiments. The imposition of condensed phase conditions on gas phase *R*-Matrix calculations,²⁸ led to the conclusion that the observed six orders of magnitude increase in DEA cross section over the calculated gas phase values¹⁴ could be explained by a *dramatic change in the survival probability of CH₃Cl[−] due to the lowering of the anion potential energy surface by polarization of the surrounding medium.*

In agreement with MS- $X\alpha$ and CMS- $X\alpha$ calculations,⁴⁵ the lowest anion state of CH₃Br[−] is found at 2.4 eV by electron transmission spectroscopy,⁴⁵ and corresponds to electron capture into the *a*₁ (σ^*) lowest unoccupied orbital. As in the case of CH₃Cl, this orbital is strongly antibonding along the CH₃–Br nuclear coordinate and the anion state is expected to dissociate into CH₃ and Br[−] fragments. One might naively expect DEA to occur at energies around 2.4 eV in gas phase experiments,^{16–26} but a Br[−] signal is observed at around 0.5 eV at room temperature due to the effect

of the survival probability factor. At higher temperatures, the DEA maximum cross section occurs near 0 eV owing to the population of higher vibrational levels of the ground electronic state²⁶ and consequent broadening of the F–C region. As mentioned previously, this latter mechanism is not effective at cryogenic temperatures and therefore cannot explain the high efficiency for CH₃ photoproduction by attachment of subvacuum electrons to CH₃Br at surfaces.^{36–38}

III. EXPERIMENT

A. Trapped charge measurements

The experimental procedure used to measure electron trapping cross sections has been described in detail elsewhere.² The technique has been developed from low energy electron transmission (LEET) spectroscopy.⁴⁶ In a LEET experiment, a magnetically collimated high resolution (0.04–0.08 eV) electron beam impinges on a multilayer-dielectric film, vacuum deposited on a metal substrate. A LEET spectrum is obtained by recording the current transmitted through the film as a function of the incident electron energy. In the spectrum, a sharp increase in the transmitted current is seen when the electrons have just enough energy to enter the film and reach the metal substrate. This increase is called the injection curve (IC). When negative charges are trapped on the surface, incoming electrons must overcome an additional repulsive barrier before being collected at the metal. A retarding potential (ΔV) thus appears at the vacuum-film interface and can be measured by the displacement of the IC to higher energies. In the past,³ it has proved useful to convert these shifts to charging rates (A_s), by measuring the repulsive potential as a function of the electron beam bombardment time (t). It has been shown that the A_s can be converted into a charging cross section (μ) as follows:³

$$A_s \equiv d\Delta V(t)/dt|_{t=0} = (LI\sigma_0/\varepsilon\pi r^2)\mu, \quad (1)$$

where L and ε are the spacer layer thickness and dielectric constant, respectively, σ_0 is in our case the methyl halide surface coverage in molecules per m²; I and r are the total current and radius of the incident electron beam.

For surface coverages smaller than unity but where molecules form clusters, the linear relationship (1) is still valid, although μ must be redefined as

$$\mu_{\text{eff}} = \sum_{n=1}^N (\sigma_n/\sigma_0)\mu_n \quad (2)$$

meaning that under these conditions, μ_{eff} corresponds to a sum of cross sections weighted by the distribution of cluster sizes ($n=1,2,\dots,N$). Here σ_n corresponds to the surface density of clusters of size n , while μ_n represents the cross section of a cluster of size n . Notice that if μ_n is independent of cluster size, then $\mu_{\text{eff}} = \bar{\mu}$ e.g., $\mu_{\text{eff}} = \bar{\mu}\sum_n n\sigma_n/\sigma_0$ and $\sum_n n\sigma_n = \sigma_0$. This is the situation expected when the surface is covered by large clusters.

CT measurements are performed with an incident electron current of typically 10^{−9} A in the 0.1–9.5 eV region. Trochoidal monochromators produce a near uniform electron

transmission function as the incident energy is increased from approximately 0.1–20 eV. This property has previously been used to study states within the band gap of Ar, N₂ and *n*-C₆H₁₄ in the energy range 0–1 eV.⁴⁷ The absolute energy scale is determined within the experimental resolution (± 0.1 eV: monochromator ± 50 meV, charging ± 50 meV) from the onset of the injection curve. Below 0.1 eV, there is a sharp decrease in incident current that corresponds to the IC itself. Useful measurements can still be obtained at these energies by normalizing the observed A_s to the appropriate incident current.

The present experimental technique is essentially that described by Marsolais *et al.*² However, it has recently been refined by improved computer control. The new data system is much more sensitive to small changes in surface potential and a ΔV as small as 1 mV is sufficient to obtain a cross section measurement. This increased sensitivity allows the cross section to be measured at several energies before the film need be replaced. The sole requirement now made, is that the total ΔV from sequential measurements be less than 50 mV as further charging distorts the IC (i.e., the charging has caused more than a simple shift in the IC). To satisfy this condition, charging times are varied in the range from 20 ms to 30 s, depending on the approximate size of the cross section. Repeated measurements are routinely required. Because the zero energy of the injection curve is not redefined for each measurement, the charging process can contribute at most a 50 meV additional uncertainty to the absolute energy scale. The smallest ΔV that can be measured per scan is 1 mV, so that the technique allows measurement of absolute trapping cross sections as low as 10^{-19} cm².

To function, the charge trapping experiment requires that the dielectric film substrate can not itself, trap electrons. This condition is satisfied for incident electron energies of less than 9.8 eV by using Kr film thicknesses of less than 50 ML. Only when molecules are added to the Kr surface can charging be observed. At larger incident energies, new channels for electron scattering become available (i.e., the formation of excitons, electron-exciton complexes and holes), and while charging (both positive and negative) continues to be observed, the interpretation of structure is more complicated.

B. Target

A platinum foil substrate press fitted to a closed cycle helium cryostat is cleaned by multiple heating at 900 K in the presence of O₂ and annealed at 1200 K. This treatment produces a reconstructed polycrystalline Pt surface whose microcrystals have azimuthal disorder with a (111) orientation.⁴⁸ Kr is known to grow layer-by-layer on such a surface forming similarly disordered microcrystals.⁴⁹ The experiments were performed at a target temperature of ~ 17 K and at a pressure of $\sim 10^{-10}$ Torr. CH₃Cl or CH₃Br molecules were physisorbed at 17 K on a multilayer Kr film condensed onto the Pt substrate.

A quadrupole mass spectrometer mounted close to the target allows the purity and quantity of gas leaked into the chamber to be monitored. Gases are introduced from a small

volume manifold via an all-metal leak valve and effuse from the end of a small tube, close to the substrate's surface. The quantity of gas leaked into the main chamber is determined by the change in pressure within the manifold as measured with a capacitance manometer. The manifold is pumped by a 8 l/s ion pump. The quantity of Kr required to form a film of given thickness can be known within 15% accuracy from monitoring the formation of quantum-size interference structures in the LEET spectrum of the film.⁴⁹ Once the Kr film is formed, a calibrated submonolayer ($\pm 30\%$) amount of the methyl halide is leaked onto its surface. The electron beam radius can be measured by moving a narrow wire (attached to a sample manipulator) through the beam. The total incident current is estimated by applying suitable potentials to the final elements of the electron gun, so that electrons initially reflected from the substrate, are repelled back into the film. Combining these uncertainties, we find a total experimental error of 50% on the absolute values of the measured cross section.

According to helium diffraction studies on graphite,⁵⁰ single layers of CH₃Cl and CH₃Br are configured in rows with alternating dipole orientation onto the (0001) face of single crystal graphite, such that a given layer is antiferroelectrically ordered and has no net dipole moment. Both molecules occupy a rectangular unit cell uniaxially commensurate with the substrate at 4.26 Å. The long edge of the unit cell is 6.38 and 6.75 Å, respectively. The photofragmentation experiments³² suggest a similar orientation on Xe(111) but helium diffraction patterns of these halides adsorbed onto a Xe(111) surface⁵⁰ at very low temperatures (10 K) indicate that the resulting deposit is poorly ordered. Since the lattice surface geometry of Kr(111) is the same as that of these substrates and the lattice parameters of Kr(111) are intermediate between *c*(0001) and Xe(111), we expect CH₃Cl and CH₃Br to form a similar unit cell configuration of intermediate size on Kr(111). We therefore used dimensions of 4.26 \times 6.5 Å to take into account the Kr lattice in our calculation of the coverage but are aware that the molecules may be disordered at 17 K.

To avoid problems associated with HCl and CCl₄ impurities in the gas-phase experiments,^{9,12} care was taken to insure that impurities could not produce detectable effects. The stated purity of the Kr gas was 99.995% and that of CH₃Cl and CH₃Br 99.5% and 99.0%, respectively. Mass spectral analysis of the methyl halides leaked into the vacuum system, with all other filaments off, indicated concentrations of HCl and CCl₄ at 4 and 6 ppm, respectively. All other contaminant levels were below 10 ppm. In the actual experiment, the filament of the electron monochromator is "on" and can *a priori* cause, (as in gas-phase experiments) degradation of the methyl halides; however, we believe that molecules are immediately condensed onto the substrate before any substantial quantity reaches the filament. To check this, halide multilayers, condensed with the filament on, were thermally desorbed and analyzed with the quadrupole mass spectrometer; no difference was observed with measurements obtained with the filament off. We also note that charge trapping cross sections we obtain are significantly dif-

ferent from those obtained for CCl₄ and other chloromethane molecules.⁵¹ Additional contamination may arise from the condensation of impurity gases and vapors onto the rare gas substrate during the course of the experiment. The effect, if any, of these on the shift ΔV , recorded in the charging experiment was estimated by measuring ΔV over the 0–10 eV range for a pure 15 ML Kr film, having left the Kr surface exposed to vacuum for an extended period of 1 h (typical experiments last less than 5 min). No significant charge was observed (i.e., $\Delta V < 0.5$ mV).

C. Charge trapping mechanisms

Several studies have already used the charge trapping method together with measurements of anion ESD, to investigate electron attachment processes in the condensed phase.^{3,28,51–55} These studies have identified mechanisms by which low energy electrons can be trapped, namely, DEA, resonance stabilization, and intermolecular stabilization. The latter, involves the trapping of very low energy electrons by a collection of molecules that are typically unable to do so in the monomeric form. In this sense, this process is similar to solvation which usually requires the reorganization of polar molecules to form a suitable trap. Intermolecular stabilization has been observed for water clusters condensed on Kr and Xe surfaces at cryogenic temperatures⁵³ presumably by the capture of charge into pre-existing traps. Both DEA and resonance stabilization involve the formation of a molecular anion. In DEA, charge is stabilized as an anionic fragment following the dissociation of the initial molecular anion. In resonance stabilization, this latter is formed in a vibrationally excited state and is itself stabilized by third body collisions. This usually requires the initial anion ground state to lie below that of the neutral molecule (e.g., O₂);³ so that the cross section for this process increases continuously with decreasing electron energy. Thus both resonance and intermolecular stabilization processes are expected to exhibit maximum electron trapping cross sections at zero electron energy with respect to the vacuum level, whereas DEA produces peaks in charge trapping cross sections at energies related to those of the transient anions. The DEA phenomenon can therefore be identified in CT experiments unless it occurs near 0 eV.

When anion ESD is not observed for a given system, charge trapping cross sections can be considered as absolute cross sections for DEA and/or resonance stabilization to the condensed molecule. Frequently, such cross sections are enhanced relative to the gas phase.^{3,52–55}

IV. RESULTS

The incident-electron energy dependence of the surface charging cross section μ for 0.1 ML of CH₃Cl condensed onto a 15 ML Kr film is shown in Fig. 1(a). The two curves (b) and (c) show the H[−] and Cl[−] ESD yield functions²⁷ for similar quantity of CH₃Cl deposited onto a 7 ML Kr film. No ESD signal was detected below 5 eV. Curve (d) in Fig. 1 is the total anion yield from the gas phase as measured by Pearl and Burrow,¹² and was obtained by subtracting a background

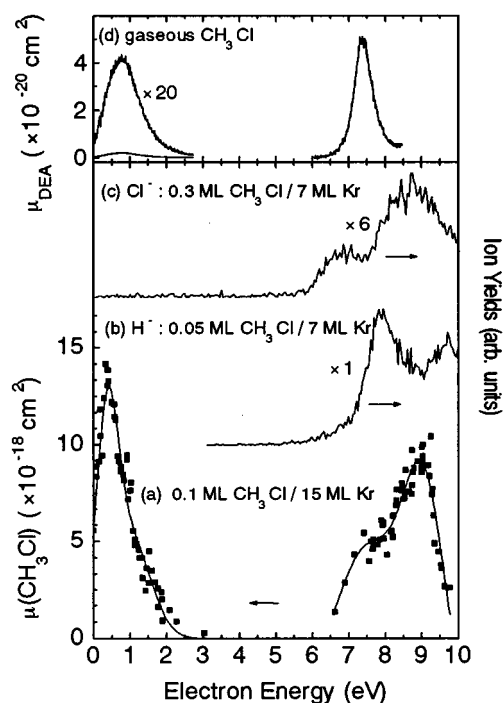


FIG. 1. Charging cross section and anion yields induced by 0–10 eV electron impact on CH₃Cl. (a) Absolute surface charging cross section for 0.1 monolayer (ML) methyl chloride condensed on a 15 ML Kr film. (b) H[−] and (c) Cl[−] desorption yields from Rowntree *et al.* (Ref. 27). (d) Total anion yield from gaseous methyl chloride as measured by Pearl and Burrow (Ref. 12).

signal at 0 eV arising from CCl₄. The 0.8 eV peak in this curve represents a cross section of $(2.0 \pm 0.4) \times 10^{-21}$ cm² for anion production, much smaller than the value of $(13 \pm 2) \times 10^{-18}$ cm² for the 0.5 eV peak in Fig. 1(a). Moreover, the origin of this gas phase structure has been questioned as its variation of magnitude with increasing temperature is consistent with the DEA of HCl.¹² The gas phase cross section for the high energy peak is $(4.9 \pm 1.0) \times 10^{-20}$ cm², a value 20 times smaller than that in the condensed phase.

The variation with Kr film thickness of the amplitude (full line) and position (dashed line) of the lowest energy CT cross section feature is shown in Fig. 2(a). Figure 2(b) presents similar measurements for the 9 eV peak. In both figures, the black squares and circles represent the experimental results, while the solid lines drawn through the error bars are intended to guide the eye. Error bars indicate the experimental uncertainty.

Figure 3 shows how charging coefficient A_s varies with incident electron energy (0–1.2 eV) for different values of CH₃Cl coverage on a 5 ML Kr film. The figure shows that with increasing coverage of CH₃Cl the position and width of the CT structure does not alter. The maximum A_s values obtained from this data and from other experiments (not shown), were used to construct Fig. 4, which illustrates how the maximum CT cross section value at 0.5 eV depends on CH₃Cl coverage.

Similar experiments were performed for CH₃Br con-

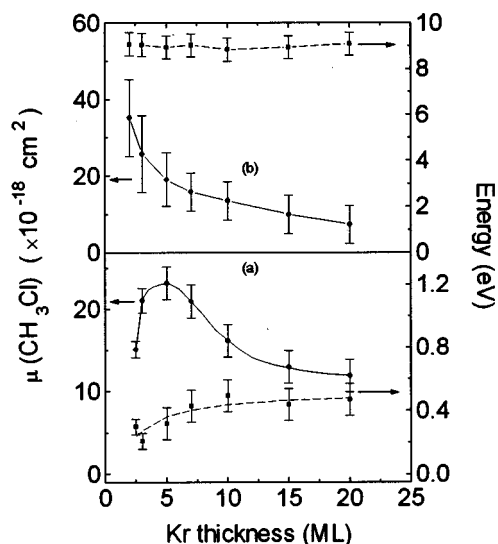


FIG. 2. Maxima in the charging cross sections of CH_3Cl and their energy position for different Kr spacer thicknesses. Results for the low energy peak, (a) and for the 9 eV peak, (b): ■—position of the maxima, ●—absolute surface charging cross section.

vibrational densed on multilayer Kr. Figure 5(a) shows how the CT cross section for 0.1 ML of CH_3Br on 15 ML of Kr, varies with incident electron energy. Two structures are clearly resolved; a maximum close to 0 eV and a broad feature that may be further resolved into two maxima at about 5.5 and 7.5 eV. For comparison, curves (c) and (d) of the same figure show the electron energy dependence of the H^- and Br^- ESD yields from 3 ML of CH_3Br .²⁷ The Br^- yield function has maxima at ~ 5 and ~ 8.5 eV whereas that for H^- desorption exhibits a maxima at 7 and 9 eV. No ESD signal was detected below 3 eV. Curve (b) represents the gas

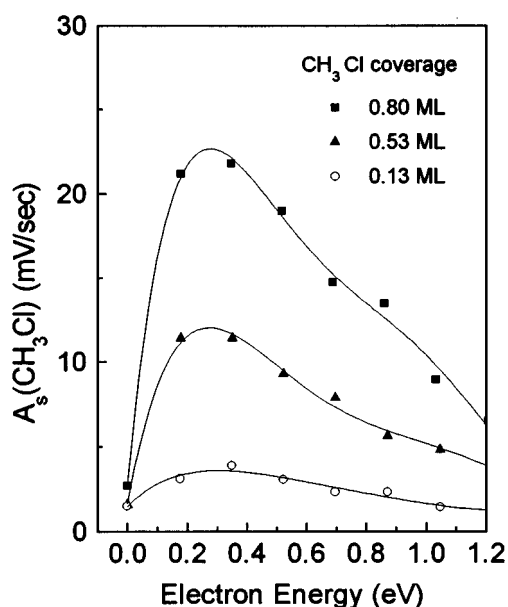


FIG. 3. Charging rates for CH_3Cl on 5 ML Kr as a function of electron energy for different CH_3Cl coverages.

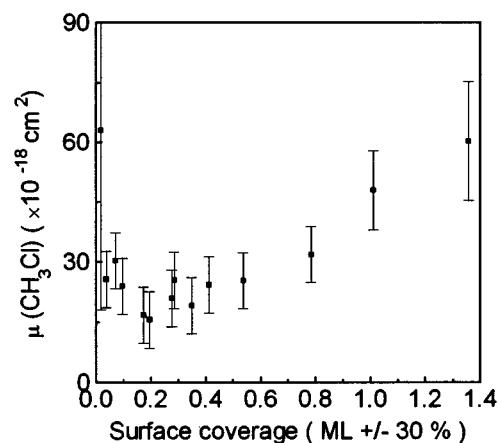


FIG. 4. Magnitude of the low energy charging cross section maximum as a function of the CH_3Cl surface coverage.

phase electron attachment cross section at low energy taken from swarm data.²⁶ The maximum cross section for Br^- production in the gas phase has a value of $1.8 \times 10^{-18} \text{ cm}^2$. This value is 150 times smaller than the peak cross section we measure at low energy (at 0.1 eV). Figure 6 shows how the magnitude and position of the maximum in the charging cross section of this latter structure varies with Kr film thickness. In Fig. 7, we illustrate how A_s in the energy range 4–9 eV, varies with Kr film thickness. For clarity, data from only three Kr film thicknesses are presented, i.e., 15, 7, and 3 ML.

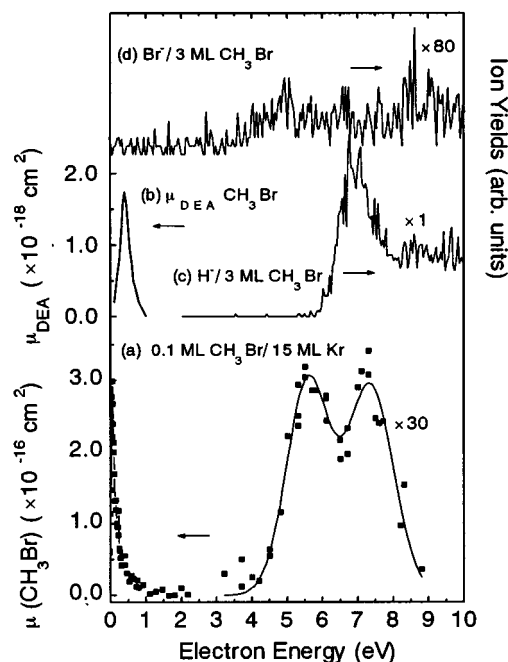


FIG. 5. Charging cross sections and anion yields induced by 0–10 eV electron impact on CH_3Br . (a) Absolute surface charging cross section for 0.1 ML methyl bromide condensed on a 15 ML Kr film. (b) Electron attachment cross section of gaseous methyl bromide in a nitrogen buffer gas as measured by Datskos *et al.* (Ref. 26). (c) H^- and (d) Br^- desorption yields from Rowntree *et al.* (Ref. 27).

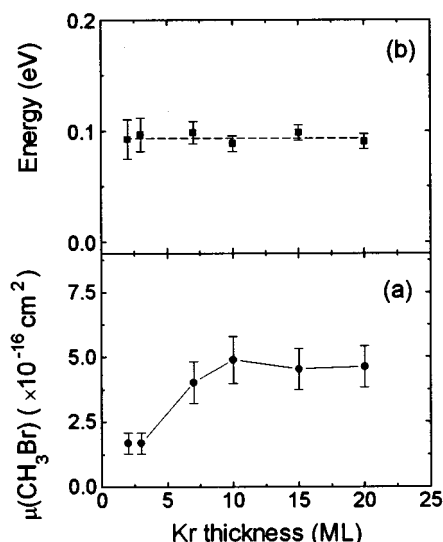


FIG. 6. (a) Maximum in the charging cross section of CH₃Br below 2 eV and (b) its energy for different Kr thicknesses: ■-position of the maxima, ●-absolute surface charging cross section.

However, data recorded at intermediate thicknesses is consistent with the data presented here. The two structures at about 5.5 and 7.7 eV in Fig. 5, display differing behavior with film thickness. Initially, A_s for both structures decreases. (The reader is reminded that μ is proportional to A_s/L , so that the observed change reflects a near constant CT cross section.) At low thicknesses (3 ML of Kr), A_s for the higher energy structure increases and the lower energy feature vanishes. The narrow energy separation of these two broad features and uncertainty about their true shape makes it difficult to provide reliable measurements for peak energies and magnitudes. The lines drawn through the data of Fig. 7 must thus be considered as guides for the eye.

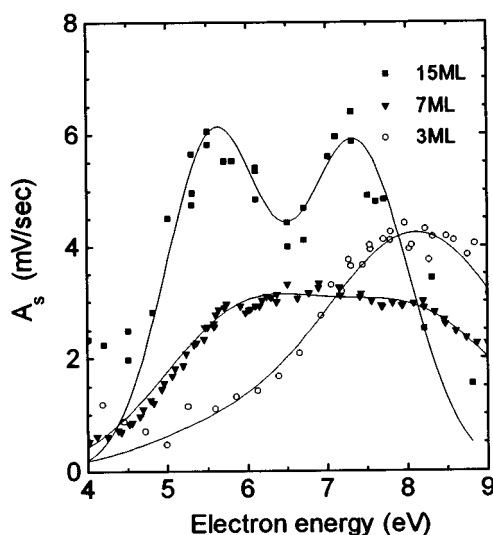


FIG. 7. Variation of charging rate (A_s) in the incident electron energy range 4–9 eV for 0.1 ML of CH₃Br on Kr films of varying thicknesses. Solid lines are drawn to guide the eye consistent with the assumption that the manifold contains two peaks of varying intensity.

V. DISCUSSION

A. Methyl chloride

The structure near 0.5 eV in Fig. 1(a), is interpreted as due to the formation of Cl[−] anions via DEA to the ²A₁ state of CH₃Cl[−] and the subsequent dissociation of Cl[−] along the strongly antibonding C–Cl[−]σ* orbital. That the DEA process involves a single scattering event at a molecule isolated on the Kr surface, is demonstrated in the data of Figs. 3 and 4. In Fig. 3, we see that increasing the surface coverage of CH₃Cl from 0.1 to 0.8 ML, does not alter the position or width of the low energy peak. Only the intensity is observed to change through this series. If charge stabilization was a two step process involving electron energy losses prior to attachment, (e.g., vibrational excitation) this peak should move to higher incident energy with increased coverage and an increased probability of energy loss. The observed behavior indicates that electrons do not lose significant energy prior to attachment. The data of Fig. 4 shows that the charge trapping cross section per molecule is independent of surface coverage below 0.6 ML. Beyond this point, μ is observed to increase with coverage and may reflect contributions from scattering processes prior to electron attachment and/or attachment to molecular aggregates. These latter might possess a larger average trapping cross section per CH₃Cl molecule due to additional intermolecular trap sites formed in a manner similar to that postulated for H₂O.⁵³ At low coverages, such as those used in our measurement of the CT cross section (i.e., 0.1 ML), the target molecules are therefore believed to be isolated from each other on the Kr surface. Hence, the measured values of μ represent the cross section from single molecules physisorbed on Kr.⁵⁶

After consideration of these points, and noting that no ESD signal is observed below 5 eV, we can conclude that for the CH₃Cl/Kr system, the charge trapping cross section represents the absolute cross section for DEA at these low energies.⁵⁶ We also note, that the maximum value of this cross section, obtained on a 5-ML-thick Kr film, (see Fig. 2) represents an enhancement over gas-phase experimental¹² and theoretical values¹⁴ of 4 and 6 orders of magnitude, respectively. As shown recently,²⁸ this dramatic enhancement and its variation with film thickness can be reproduced with *R*-Matrix calculations that include a simple model of the effect of the local polarization on the DEA process. Using the most basic elements of that model, we now explain the present results.

At first sight, it may not be obvious that DEA seen below 1 eV in the present experiment arises from a resonance of σ symmetry that appears at ~3.5 eV in the gas phase excitation function of C–Cl stretch modes.^{14,15,41–43} However, Fig. 8(b) shows schematic potential energy curves for neutral methyl chloride and for the anion state in condensed and gas phases. Panels 8(b) and 8(c) show that the vibrational excitation of the ν_3 stretch mode,⁴³ for example, is initiated by temporary attachment of the electron to neutral methyl chloride to form a transient negative ion that rapidly autoionizes. The lifetime of this anion is extremely short ($\tau \sim 10^{-15}$ s) in the gas phase and thus only the first few

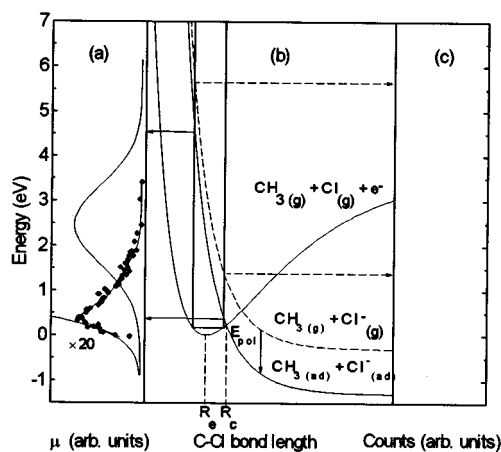


FIG. 8. Proposed mechanism for dissociative electron attachment to condensed phase CH_3Cl . Panel (a): experimental data (dots) and proposed shape of condensed phase vibrational excitation function of CH_3Cl . Panel (b): potential curves of neutral methyl chloride, of the lowest anion state (2A_1) in the gas phase and of the latter shifted down by 1 eV to approximate the effect of the polarized substrate. Panel (c): relative excitation function for the ν_3 vibrational mode of methyl chloride (Ref. 43).

vibrational levels are excited⁴³ and little dissociation is expected.

In contrast, our measurements indicate that for the condensed molecule, DEA is strongly enhanced. Similar, though smaller enhancements in DEA have been observed in other systems^{3,51–55} and have been understood as deriving from the effects of image charges which are induced in the film and in its metal substrate by anions at the film's surface.⁵⁷ The resulting charge/image charge attraction has two primary effects:

- (i) A potential energy barrier to anion desorption is created, the height of which is equal to E_p the surface polarization energy. For this reason, the kinetic energies of desorbed ions are lower than those seen in comparable gas phase DEA experiments.^{58,59}
- (ii) The potential energy (PE) surface of the intermediate anion state formed at the film surface, is shifted to lower energy by E_p . As a consequence, electron attachment from the neutral ground state can be achieved using electrons of lower energy than that necessary for gas phase DEA.³ This is represented in Fig. 8(b) by shifting the negative ion curve down by the polarization energy of the krypton surface, approximately 1 eV.⁶⁰

The enhancement in the DEA cross section is a further result of this latter process. The cross section depends not only on the probability that the intermediate anion is formed, but also on the probability that the anion survives (termed “survival factor”) until dissociation is irreversible. This latter condition is satisfied once the internuclear separation along the dissociation coordinate is greater than R_c , the crossing point of the intermediate anion, and the neutral ground-state PE surfaces (along the dissociation coordinate). The DEA cross section will thus depend on the ratio of the anion's lifetime to the “transit time” required for it to relax

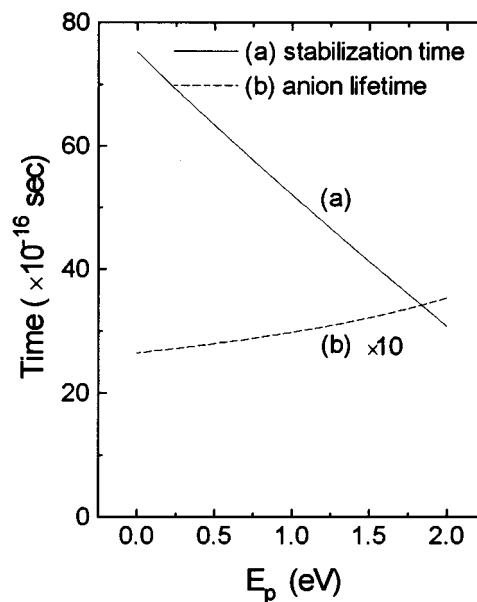


FIG. 9. Variation of classical transit time from the equilibrium $\text{CH}_3\text{-Cl}$ separation (R_e) to the anion/ground state crossing point, and anion lifetime for electron attachment at R_e , as functions of surface polarization energy (which is assumed equal to the anion PE curve shift).

to R_c .⁶¹ Lowering the PE surface of CH_3Cl^- brings R_c closer to the equilibrium separation of the neutral molecule R_e . Thus, less time is required for the nuclei of the intermediate anion to travel from the F–C region into the stabilization region. Additionally, as the anion PE surface is lowered, the decay probability per unit time (or the resonance width) at a particular internuclear separation decreases. Both effects lead to a dramatic increase in the survival factor.

To illustrate the relative importance of these effects, the anion lifetime for attachment at R_e and the classical transit time for traveling between R_e and R_c were calculated using the R -matrix model²⁸ and the anion PE curve, as functions of the anion curve shift (E_p). The results are shown in Fig. 9. These curves serve only for illustrative purposes as the DEA dynamics are determined by a complicated combination of different factors including the Franck–Condon overlap and the dependence of the resonance width on the internuclear distance. In particular, the capture into the resonance state occurs at internuclear distances which are somewhat greater than R_e . Nevertheless, we observe that although both transit time and anion lifetime are affected by a change in polarization, the effect is greater on the transit time. Moreover, as the film thickness decreases, the effective potential for electron motion in the resonance state loses the spherical symmetry and the resonance state increases its admixture of $l=0$ component. This decreases the resonance lifetime. Thus, as Gerber and Herzenberg⁶² note for an anion resonance close to a surface, the image potential which lowers the energy of the electron inside the core and which alone would strengthen the effective tunneling barrier, has the net result of broadening the resonance as its effect is substantially stronger outside the core than inside. So although we are not presently in a position to make any quantitative estimates for methyl

chloride, it appears that the reduction of the transit time is the dominant factor leading to the observed increase in the DEA cross section.

In the condensed phase, when an electron attaches to methyl chloride with more than 2 eV, the transient negative ion lifetime is so short that the electron will autodetach before dissociation leaving the molecule in an excited vibrational mode of the C–Cl bond (electrons of higher incident energies, may allow this resonance to decay and excite the ν_4^{CH} stretch mode, the excitation function of which shows a maximum at 5 eV).⁴³ The effect of surface polarization is illustrated in panel (a) of Fig. 8, which shows both the expected condensed phase vibrational excitation function for the ν_3 stretch mode (the Gaussian curve) and the CT cross section (circles). Dissociation occurs on the low energy tail of the resonance, where cleavage of the C–Cl bond and the formation of Cl[−] anions is not prevented by the short lifetime of the CH₃Cl[−] state.

As the thickness L of the Kr film is reduced, so is the distance between the metal and anions on the film surface. In the simplest models, the polarization energy increases from its thick film limit, (~ 1 eV at 16 ML Kr) with an approximately $1/L$ dependence.⁵⁷ The experimental variation in DEA peak position and magnitude is depicted in Fig. 2(a): the peak shifts to lower energy with an increase of polarization energy. This variation is modeled in the figure by the dashed line that follows an equation of the same form used to describe changes in the energy of the $^2\Pi_u$ resonance of N₂[−] on Kr films.⁵⁷ Increasing E_p is also seen to increase the DEA cross section [full line in Fig. 2(a)]. This behavior can be explained by the reduction in the Kr thickness which causes the anion PE curve (Fig. 8) to shift to lower energy and brings the crossing point R_c closer to the equilibrium separation R_e . The time required to stabilize an anion is further reduced and increases the DEA cross section.

The cross section reaches its highest value on a 5 ML-thick Kr film. Further decreasing the Kr film thickness reduces the DEA signal despite the increase in E_p as indicated by changes in the position of the DEA peak. This decrease in DEA cross section could perhaps be ascribed to changes in two resonance parameters; a decrease in the anion lifetime (due to modification of the partial wave content of the state and to the opening of new decay channels from the metal) and to a shift of the threshold of the electron continuum to lower energies due to the electron-metal interaction.²⁸ This latter modification shifts the PE surface of the neutral molecule downwards. If the shift of the anion curve due to the presence of the metal were smaller than that of the ground state of the neutral molecule, the greater separation between the negative ion and the neutral curves would reduce the DEA cross section. Problems arise with this model as from a classical viewpoint, the molecular anion better presents a point charge than does the incident electron and thus should feel to a greater extent the effects of substrate polarization. Consequently, we would expect any shift of the neutral curve will be less than that of the anion curve. Moreover, the threshold of the electron continuum is determined by V_0 (the lowest allowed energy of an electron within the film) which

has been observed constant for $L > 3$ ML.⁴⁹ Thus, while a suitably strong electron-metal interaction may perhaps explain a decrease in DEA below 2 or 3 ML it can not account for the observed decrease in cross section for films as thick as 5 ML.

The reduction of anion lifetime (and hence DEA), that has been predicted⁶³ and observed⁵⁷ to occur for negative ion resonances close to a metal substrate, originates from the increase of the overlap between the electron wave function derived from electron-image charge potential and that describing the intermediate negative-ion state. Thus, the anion itself decays by tunneling to states above the Fermi level of the metal. Theoretical studies⁶³ have shown that this effect only becomes important at film thicknesses < 7 a.u. (or about 2 ML) i.e., smaller distances than those studied here. Experimental studies of the vibrational excitation of N₂⁵⁷ exhibit a somewhat stronger effect than that predicted by theory which might derive from the aforementioned change of symmetry of the resonance due to the electron-surface interaction. However, attempts to reproduce the present experimental data by an additional increase of the width failed and so its functional form was kept constant in the calculations of Ref. 28. Of course, quantitative investigation of the symmetry-change effect should be made in future calculations.⁶⁴

Given that changes to the anion lifetime and electron-metal interaction are believed only to appear or become possible for $L < 2$ or 3 ML, we propose in a qualitative manner, another mechanism that could start reducing the DEA cross section at 5 ML. Previous studies from this laboratory have indicated the decisive role of the electron density of states in the scattering of low energy electrons by condensed systems.⁶⁵ It is possible that the observed reduction in DEA cross section below 5 ML is due to the comparatively high density of states in the metal which enhances electron transfer to the Pt substrate. In essence, an electron hops directly to the metal rather than attach to the molecular target. The two processes represent competing channels and so decreases in the effective *electron capture cross section* of the molecule and hence DEA, are observed. The efficiency of the “hopping” process would vary with film thickness and would be sensitive to the physical extent of the electronic wave packet. We believe it significant that a Kr film thickness of 5 ML (or 1.7 nm) is approximately the same size as the DeBroglie wavelength of a 0.5 eV electron. Below 5 ML film thickness, the electron has an enhanced probability of passing through the spacer layer to the metal, within its time of interaction with the adsorbed molecule.

The two structures seen at higher energy (7.5 and 9.0 eV) in the CT cross section, are consistent with the ESD anion yields²⁷ shown in Fig. 1, considering that the charging threshold occurs at lower incident electron energy than those for ESD. This shift is most likely due to the effects of the surface polarization. The H[−] yield from CH₃Cl on a multilayer Kr film peaks at 8.0 and 9.8 eV, the Cl[−] signal shows peaks at 6.7 and 8.7 eV.²⁷ It would be tempting, on the basis of the energy separation between doublet structures, to suggest that the charge trapping cross section was most strongly correlated to H[−] production. However, it is quite

probable that the desorption probabilities for the two anions are different and vary with incident electron energy⁶⁶ so that the contributions of different anions to the charging cross section *can not* be isolated. We note that the 9.8 eV structure in H⁻ ESD signal is associated with increased ion production via charge/energy transfer from Kr^{*-}.⁶⁷ If significant quantities of H⁻ so formed are trapped, a peak should appear at this energy in the charge trapping cross section. That no structure is seen at this energy, suggests two possibilities; that significant quantities of H⁻ do not trap or that the CT measurement does not reflect anion formation accurately in this energy range. Recent calculations and unpublished data indicate that the first possibility is often true for organic molecules.⁶⁶ However, we must note that the CT cross section drops more quickly from its maximum value at 9 eV than do either of the anion yields, indicating that the shape of the CT cross section at these energies may be determined by factors other than anion production. In particular, we have noticed that undoped Kr films can charge positively at incident energies greater than the first exciton, but less than that necessary for direct ionization to Kr⁺, possibly from fusion of Kr^{*} excitons.⁶⁸

Due to its low intensity, the variation of the 7.5 eV feature with spacer thickness has not been measured. The cross section behavior of the 9.0 eV structure depicted in Fig. 2(b) by the full line, is similar to that reported in panel (a) for the resonance at 0.5 eV for Kr thicknesses larger than 7 ML, but continues to rise below this thickness. We therefore expect that the cross section be enhanced relative to the gas phase in a manner similar to that described for the case of the ²A₁ state of CH₃Cl⁻. However, in the present case, the enhancement would be obtained by the polarization shift of the anion PE surface relative to those of neutral *excited* states, into which the anion would normally decay.³ As before, the polarization and cross section enhancement, should increase with decreasing film thickness. That no reduction in cross section is observed for Kr film thicknesses >3 ML is consistent with the suggested mechanism for a reduction in electron capture cross section and reflects the shorter range of the interaction of a 9 eV electron with the metal substrate. The DeBroglie wavelength of a 9.0 eV electron is much smaller than that of a 0.5 eV electron and competition from transfer to the metal could only become significant at thicknesses <1 ML.

We must also consider that the stable anion created by the higher energy CH₃Cl states can escape into vacuum and that decreasing the Kr film thickness produces an increase in the potential barrier that must be overcome for charged species to escape the film. This results in a larger fraction of the ion fragments staying on the surface and to an increase in the surface charging cross section. Determining the fraction of ions that desorb is difficult, but previously has been thought to be small for O⁻ from O₂⁵² and F⁻ from CF₄ (i.e., <30%).⁵⁴ If the same were true for ESD from CH₃Cl, then this explanation for the variation of cross section could be discounted. However, the desorption probability of an ion depends on the available kinetic energy, which itself is dependent on the anion's PE surface and on the relative mass of the fragment ion and neutral molecule. The energy avail-

able to a light H⁻ ion could be considerably greater than that available to a Cl⁻ ion (or O⁻ and F⁻ in the previous examples). It is thus possible that this mechanism contributes to the variation in CT cross section shown in Fig. 2(b).

The energy of the 9 eV feature is not observed to alter with changes in film thickness, [dashed line in Fig. 2(b)] which suggests a surprising insensitivity to changes in polarization. However, it is possible that the CT data above 9 eV contains contributions from processes occurring in the Kr film and that the true maximum value and energy of this feature are not seen in the present experiment.

B. Methyl bromide

Methyl bromide is much like methyl chloride as regards the symmetry assignment of its anion states. Comparisons between Figs. 1 and 6 lead one to conclude that the processes responsible for surface charging are similarly related. Moreover, before proceeding in this discussion, we note that measurements of the variation of CT cross section with CH₃Br coverage (not shown) indicate that as for CH₃Cl (see Figs. 3 and 4), trapping proceeds via attachment to isolated molecules (at coverages <0.4 ML) without prior energy loss.

As in the case of CH₃Cl, the lowest energy feature seen at 0 eV can be interpreted as due to DEA via the lowest ²A₁ anion state. Both CMS-*Xα* calculations⁴⁵ and ETS experiments⁴⁵ at room temperature place this state in the 2.0–2.5 eV energy range. However, the associated DEA should be expected to appear at lower energy in the condensed phase because of the effects of surface polarization and the state's short lifetime on the survival probability as explained in the previous section for CH₃Cl. As no anions are observed to desorb for incident energies <3 eV,²⁷ our measurements represent a total absolute cross section for DEA via the ²A₁ state. Once more, this cross section is significantly larger than comparable gas phase measurements; the CT cross section at 0 eV in Fig. 5(a) is more than 150 times larger than that recorded by Datskos *et al.*²⁶ at 0.38 eV [in (d)] for the gas phase CH₃Br at 300 K. Furthermore, our measurements provide only a minimum estimate of the cross section enhancement, since the maximum in the DEA cross section may lie below 0 eV. In this case, the largest charging cross section could be obtained with subvacuum electrons, as produced in photoelectron experiments. This hypothesis is consistent with the observation that the position of low energy DEA peak does not change with film thickness [Fig. 6(a)], as we observe only the high energy tail of the DEA process, the maximum of which always remains at 0 eV. Due to the low energy cut off, the cross sections reported in Fig. 4(a) should be treated as a lower limit for the total absolute condensed phase DEA *peak* cross section. Thus, our measurements represent an increase over the gas phase values of *at least* two orders of magnitude.

The decrease seen in the CT cross section at 0 eV for film thicknesses less than 10 ML, is reminiscent of that seen for CH₃Cl below 5 ML. We believe the observed behavior reflects a greater probability for transfer of the electron directly to the metal and a consequent reduction in that elec-

tron capture cross section at greater Kr film thicknesses. Again, we note that the Kr thickness at which a reduction in the DEA cross section is first observed (10 ML) corresponds roughly to the extent of the DeBroglie wave length of a 0.1 eV electron.

It seems clear from Figs. 5 and 7, that the 4–10 eV charging manifold contains contributions from at least two states, the clearest features appearing at ~ 5.5 and 7.7 eV. From comparison with the ESD of H[−] and Br[−] in Fig. 5, we interpret these features as due to surface charging via DEA. It is difficult to determine how the CT cross section of these features varies with Kr film thickness as they are poorly resolved, the data contain noise and their exact shape is unknown for fitting purposes. However, certain observations can be made. For example, Fig. 7 shows that A_s for the lower energy feature decreases with decreasing Kr thickness L , (down to 7 ML). Recall from Eq. (1), that A_s is proportional to L , so that the observed decrease in A_s corresponds to a near constant CT cross section. Coefficient A_s for the higher energy feature initially decreases, but increases at small (< 7 ML) thicknesses. This accords with a near constant CT cross section as L is reduced from 15 to 7 ML and then a significant increase, (by an order of magnitude over the thick film value), as the Kr film is reduced to 2 ML. The apparent disappearance of the low energy feature on films of less than 7 ML is consistent with its signature being “swamped” by changes in the cross section of the higher energy feature. This increase in cross section is most likely due to mechanisms of the type already discussed for CH₃Cl, namely, an increased survival probability and/or decreases in desorption. Both these mechanisms are of course, related to the increase in polarization energy of the thinner films.

VI. CONCLUSIONS

The charge trapping cross section has been measured for CH₃Cl and CH₃Br physisorbed on multilayer Kr condensed on a Pt substrate. Features observed in the 0–10 eV incident electron energy range result from DEA to different parent anion states and find counterparts in data from either the gas phase or condensed phase ESD. By measuring charging rates at low energy (< 1.5 eV) for various surface coverages of the methyl halide compounds, we have showed that the DEA behavior is that of molecules isolated from each other, for coverages less than 0.6 ± 0.2 and 0.4 ± 0.2 ML for methyl chloride and methyl bromide, respectively. At higher coverages, a larger cross section “per target molecule” is observed and results probably from an increased DEA cross section for clustered molecules.

On thick Kr layers, where the polarization energy depends purely on the dielectric properties of the film, we measured the peak charging cross sections to be 13×10^{-18} and 9×10^{-18} cm² $\pm 50\%$ for the 0.5 and the 9.0 eV features of CH₃Cl, respectively. For the same conditions, the peak cross sections for CH₃Br are 3.0×10^{-16} , 10×10^{-18} , and 10×10^{-18} cm² for the 0.1, 5.5, and 7.7 eV features. (All cross sections $\pm 50\%$) The values below 5 eV represent total absolute condensed phase DEA cross sections, whereas the

values at higher energies set lower limits for DEA.

The measured condensed phase cross sections are enhanced significantly relative to gas phase values. This enhancement is attributed to a shift to lower energy of the potential energy surfaces of intermediate anions, caused by the polarization of the Kr/Pt substrate. This shift, in turn increases the survival probability factor of ions to dissociate.

We propose that reducing the thickness of the Kr film has two principal effects:

- An increase in polarization energy that further lowers the intermediate anion PES and increases survival probability.
- (b) An increase in the probability of electron transfer directly to the Pt substrate which reduces the capture probability of the molecule and hence DEA.

The point at which mechanism (b) will become sufficient to reduce the DEA (or CT) cross section will depend on the spatial extent of the incident electron wave function which increases with decreasing electron energy. As a consequence, a reduction in DEA and CT cross section is observed for the two low lying ²A₁ anion states of CH₃Br and CH₃Cl at Kr thicknesses corresponding roughly to the DeBroglie wavelengths of incident electrons. In contrast, for both molecules, the highest lying anion states show only an increase in the CT cross section with decreasing Kr film thickness.

ACKNOWLEDGMENTS

This work has been funded by the Natural Science and Engineering Council (NSERC) of Canada and by Hydro-Quebec. P.A. wishes to thank NSERC for financial support. I.I.F. is grateful to L.S. and members of his group for financial support and hospitality during his stay at the University of Sherbrooke. I.I.F. has been supported by the U.S. National Science Foundation through Grant No. PHY-9509265.

¹G. J. Schulz, *Rev. Mod. Phys.* **45**, 423 (1973).

²R. M. Marsolais, M. Deschênes, and L. Sanche, *Rev. Sci. Instrum.* **60**, 2724 (1989).

³L. Sanche and M. Deschênes, *Phys. Rev. Lett.* **61**, 2096 (1988).

⁴L. Sanche, in *DIET III*, edited by R. H. Stulen and M. L. Knotek (Springer, Berlin, 1988), Chap. 6.

⁵L. Sanche, in *DIET V*, edited by A. R. Burns, E. B. Stechel, and D. R. Jennison (Springer, Berlin, 1993), Chap. 1.

⁶Z. L. Petrovic, W. C. Wang, and L. G. Lee, *J. Chem. Phys.* **90**, 3145 (1989).

⁷S. K. Srivastava and O. J. Orient, in *Proceedings of the 3rd Int. Symposium on the Production and Neutralization of Negative Ions and Beams*, Brookhaven, 1983, edited by K. Prelic, American Institute of Physics, 1984 (unpublished).

⁸P. G. Datskos, L. G. Christophorou, and J. G. Carter, *Chem. Phys. Lett.* **168**, 324 (1990).

⁹S. C. Chu and P. D. Burrow, *Chem. Phys. Lett.* **172**, 17 (1990).

¹⁰H.-U. Scheunemann, E. Illenberger, and H. Baumgartel, *Ber. Bunsenges. Phys. Chem.* **84**, 580 (1980).

¹¹F. H. Dorman, *J. Chem. Phys.* **44**, 3856 (1966).

¹²D. M. Pearl and P. D. Burrow, *Chem. Phys. Lett.* **206**, 483 (1993).

¹³D. M. Pearl and P. D. Burrow, *J. Chem. Phys.* **101**, 2940 (1994).

¹⁴I. I. Fabrikant, *J. Phys. B At. Mol. Opt. Phys.* **24**, 2213 (1991); *ibid.* **27**, 4325 (1994).

¹⁵D. M. Pearl, P. D. Burrow, I. I. Fabrikant, and G. A. Gallup, *J. Chem. Phys.* **102**, 2737 (1995).

¹⁶D. Spence and G. J. Schulz, *J. Chem. Phys.* **58**, 1800 (1973).

- ¹⁷Measurements of T. G. Lee, *J. Phys. Chem.* **67**, 360 (1963); analyzed by R. P. Blaunstein and L. G. Christophorou, *J. Chem. Phys.* **49**, 1529 (1968).
- ¹⁸E. Alge, N. G. Adams, and D. Smith, *J. Phys. B At. Mol. Phys.* **17**, 3827 (1984).
- ¹⁹I. Szamrej, H. Kosci, B. M. Forsys, B. Zytomirski, and B. G. Dzantijew, *Radiat. Phys. Chem.* **38**, 541 (1991).
- ²⁰K. G. Mothes, E. Schultes, and R. N. Schindler, *J. Phys. Chem.* **76**, 3758 (1972).
- ²¹K. M. Bansal and R. W. Fessenden, *Chem. Phys. Lett.* **15**, 21 (1972).
- ²²Z. L. Petrovic and R. W. Crompton, *J. Phys. B At. Mol. Phys.* **20**, 5557 (1987).
- ²³A. A. Christodoulides and L. G. Christophorou, *J. Chem. Phys.* **54**, 4691 (1971).
- ²⁴J. A. Stockdale, F. J. Davis, R. N. Compton, and C. E. Klotz, *J. Chem. Phys.* **60**, 4279 (1974).
- ²⁵W. C. Wang and L. C. Lee, *J. Appl. Phys.* **63**, 4905 (1988).
- ²⁶P. G. Datskos, L. G. Christophorou, and J. G. Carter, *J. Chem. Phys.* **97**, 9031 (1992).
- ²⁷P. Rowntree, L. Sanche, L. Parenteau, M. Meinke, F. Weik, and E. Illenberger, *J. Chem. Phys.* **101**, 4248 (1994).
- ²⁸L. Sanche, A. D. Bass, P. Ayotte, and I. I. Fabrikant, *Phys. Rev. Lett.* **75**, 3568 (1995).
- ²⁹E. P. March, T. L. Gilton, W. Meier, M. R. Schneider, and J. P. Cowin, *Phys. Rev. Lett.* **61**, 2725 (1988).
- ³⁰S. K. Jo and J. M. White, *J. Phys. Chem.* **94**, 6852 (1990).
- ³¹F. Solymosi, J. Kiss, and K. Révész, *J. Chem. Phys.* **94**, 8510 (1991).
- ³²E. P. Marsh, F. L. Tabares, M. R. Schneider, T. L. Gilton, W. Meier, and J. P. Cowin, *J. Chem. Phys.* **92**, 2004 (1990).
- ³³X.-L. Zhou and J. M. White, *Chem. Phys. Lett.* **167**, 205 (1990).
- ³⁴T. L. Gilton, C. D. Dehnhostel, and J. P. Cowin, *J. Chem. Phys.* **91**, 1937 (1989).
- ³⁵S.-A. Costello, B. Roop, Z.-M. Liu, and J.-M. White, *J. Chem. Phys.* **92**, 1019 (1988).
- ³⁶V. A. Ukraintsev, T. J. Long, T. Gowl, and I. Harrison, *J. Chem. Phys.* **96**, 9114 (1992).
- ³⁷V. A. Ukraintsev, T. J. Long, and I. Harrison, *J. Chem. Phys.* **96**, 3957 (1992).
- ³⁸V. A. Ukraintsev and I. Harrison, *J. Chem. Phys.* **98**, 5971 (1993).
- ³⁹St. J. Dixon-Warren, D. V. Heyd, E. T. Jensen, and J. C. Polanyi, *J. Chem. Phys.* **98**, 5938, 5954 (1993).
- ⁴⁰Q. Y. Yang, W. N. Schwarz, and R. M. Osgood, Jr., *J. Chem. Phys.* **98**, 10 085 (1993).
- ⁴¹P. D. Burrow, A. Modelli, N. S. Chiu, and K. D. Jordan, *J. Chem. Phys.* **77**, 2699 (1982).
- ⁴²M. Guerra, D. Jones, G. Distefano, F. Scagnolari, and A. Modelli, *J. Chem. Phys.* **94**, 484 (1991).
- ⁴³X. Shi, T. M. Stephen, and P. D. Burrow, *J. Chem. Phys.* **96**, 4037 (1992); X. Shi, U. K. Chan, G. A. Gallup, and P. D. Burrow, *ibid.* **104**, 1855 (1996).
- ⁴⁴M. Falcetta and K. D. Jordan, *J. Phys. Chem.* **94**, 5666 (1990).
- ⁴⁵A. Modelli, F. Scagnolari, G. Distefano, D. Jones, and M. Guerra, *J. Chem. Phys.* **96**, 2061 (1992).
- ⁴⁶L. Sanche, *J. Chem. Phys.* **71**, 4860 (1979).
- ⁴⁷L. G. Caron, G. Perluzzo, G. Bader, and L. Sanche, *Phys. Rev. B* **33**, 3027 (1986).
- ⁴⁸C. Gaubert, R. Baudoing, Y. Gauthier, M. Michaud, and L. Sanche, *Appl. Surf. Sci.* **25**, 195 (1986).
- ⁴⁹G. Perluzzo, G. Bader, L. G. Caron, and L. Sanche, *Phys. Rev. Lett.* **55**, 545 (1985).
- ⁵⁰P. A. Rowntree, G. Scoles, and J. C. Ruiz-Suárez, *J. Phys. Chem.* **94**, 8511 (1990).
- ⁵¹A. D. Bass, J. Gamache, P. Ayotte, and L. Sanche, *J. Chem. Phys.* **104**, 4258 (1996).
- ⁵²H. Sambe, D. E. Ramaker, M. Deschênes, A. D. Bass, and L. Sanche, *Phys. Rev. Lett.* **64**, 523 (1990).
- ⁵³A. D. Bass and L. Sanche, *J. Chem. Phys.* **95**, 2910 (1991).
- ⁵⁴A. D. Bass, J. Gamache, L. Parenteau, and L. Sanche, *J. Phys. Chem.* **99**, 6123 (1995).
- ⁵⁵M. A. Huels, A. D. Bass, P. Ayotte, and L. Sanche, *Chem. Phys. Lett.* **245**, 387 (1995).
- ⁵⁶We do not believe that for this system, resonance stabilization contributes to charging. Stable CH₃Cl is not observed in the gas phase and the potential energy surface of the anion (see Ref. 14) appears purely repulsive.
- ⁵⁷M. Michaud and L. Sanche, *J. Electron Spectrosc. Relat. Phenom.* **51**, 237 (1990).
- ⁵⁸M. Meinke, L. Parenteau, P. Rowntree, L. Sanche, and E. Illenberger, *Chem. Phys. Lett.* **205**, 213 (1993).
- ⁵⁹M. A. Huels, L. Parenteau, M. Michaud, and L. Sanche, *Phys. Rev. A* **51**, 337 (1995).
- ⁶⁰The surface polarization energy induced by a transient anion has been measured previously. For N₂⁻ (²Π_g) found on relatively thick (>15 ML) Kr film, it was measured to be 0.72 eV,⁵⁷ whereas for O₂⁻ (²Π_u) sitting on 20 ML of Kr a value of 0.9 eV was deduced from comparison with theory.³ In fact, the surface polarization energy will vary slightly with adsorbed species because it depends on the charge density and on the distance at which charge resides from the surface as well as the dielectric constant of the film. We have found that E_p is frequently of the order of 1 eV.
- ⁶¹See, for example, T. F. O Malley, *Phys. Rev.* **150**, 14 (1966).
- ⁶²A. Gerber and A. Herzenberg, *Phys. Rev. B* **31**, 6219 (1985).
- ⁶³D. Teillet-Billy, V. Djamo, and J. P. Gauyacq, *Surf. Sci.* **269/270**, 425 (1992); P. J. Rous, *ibid.* **260**, 361 (1992); D. Teillet-Billy and J. P. Gauyacq, *ibid.* **239**, 343 (1990); J. P. Gauyacq, V. Djamo, and D. Teillet-Billy, in *Electronic and Atomic Collisions, XVII ICPEAC*, edited by W. R. McGillivray, I. E. McCarthy, and M. C. Standage (IOP Publishing, Bristol, 1992) p. 243.
- ⁶⁴For low-energy electrons, the rigorous description of this effect is complicated by the fact that the electron wavefunction in the far region is dominated by the *s* wave. In particular, the behavior of the width in the low-energy region is determined by the *s* wave Wigner exponent modified by the dipolar interaction [for example see I. I. Fabrikant, *Sov. Phys. JETP* **46**, 693 (1977); W. Domcke and L. S. Cederbaum, *J. Phys. B* **14**, 149 (1981)]. Only when the electron approaches the molecule and is captured into the resonance state, is the wavefunction dominated by the *p* wave.
- ⁶⁵M. Michaud, L. Sanche, T. Goulet, and J.-P. Jay-Gerin, *Phys. Rev. Lett.* **66**, 1930 (1991); M. Michaud, P. Cloutier, and L. Sanche, *Phys. Rev. B* **44**, 10 485 (1991-I).
- ⁶⁶A. D. Bass and L. Sanche (unpublished).
- ⁶⁷M. Michaud, P. Cloutier, and L. Sanche, *Phys. Rev. B* **11**, 336 (1993-I); P. Rowntree, H. Sambe, L. Parenteau, and L. Sanche, *Phys. Rev. B* **47**, 4537 (1993 II).
- ⁶⁸P. Ayotte (private communication).